Tensor Forces and the Ground-State Structure of Nuclei

R. Schiavilla,[1,2] R. B. Wiringa,[3] Steven C. Pieper,[3] and J. Carlson[4]

[1]*Jefferson Laboratory, Newport News, Virginia 23606, USA*
[2]*Department of Physics, Old Dominion University, Norfolk, Virginia 23529, USA*
[3]*Physics Division, Argonne National Laboratory, Argonne, Illinois 61801, USA*
[4]*Theoretical Division, Los Alamos National Laboratory, Los Alamos, New Mexico 87545, USA*

Two-nucleon momentum distributions are calculated for the ground states of nuclei with mass number $A \leq 8$, using variational Monte Carlo wave functions derived from a realistic Hamiltonian with two- and three-nucleon potentials. The momentum distribution of np pairs is found to be much larger than that of pp pairs for values of the relative momentum in the range (300–600) MeV/c and vanishing total momentum. This order of magnitude difference is seen in all nuclei considered and has a universal character originating from the tensor components present in any realistic nucleon-nucleon potential. The correlations induced by the tensor force strongly influence the structure of np pairs, which are predominantly in deuteronlike states, while they are ineffective for pp pairs, which are mostly in $^1S_0$ states. These features should be easily observable in two-nucleon knockout processes, such as $A(e, e'np)$ and $A(e, e'pp)$.

The two preeminent features of the nucleon-nucleon (*NN*) interaction are its short-range repulsion and intermediate- to long-range tensor character. These induce strong spatial-spin-isospin *NN* correlations, which leave their imprint on the structure of ground- and excited-state wave functions. Several nuclear properties reflect the presence of these features. For example, the two-nucleon density distributions $\rho_{TS}^{M_S}(\mathbf{r})$ in states with pair spin $S = 1$ and isospin $T = 0$ are very small at small internucleon separation $\mathbf{r}$ and exhibit strong anisotropies depending on the spin projection M_S [1]. Nucleon momentum distributions $N(k)$ [2,3] and spectral functions $S(k, E)$ [4] have large high-momentum and, in the case of $S(k, E)$, high-energy components, which are produced by short-range and tensor correlations. The latter also influence the distribution of strength in response functions $R(k, \omega)$, which characterize the response of the nucleus to a spin-isospin disturbance injecting momentum $\mathbf{k}$ and energy ω into the system [5,6]. Lastly, calculations of low-energy spectra in light nuclei (up to mass number $A = 10$) have demonstrated that tensor forces play a crucial role in reproducing the observed

ordering of the levels and, in particular, the observed absence of stable $A = 8$ nuclei [7].

In the present study we show that tensor correlations also impact strongly the momentum distributions of *NN* pairs in the ground state of a nucleus and, in particular, that they lead to large differences in the np versus pp distributions at moderate values of the relative momentum in the pair. These differences should be observable in two-nucleon knockout processes, such as $A(e, e'np)$ and $A(e, e'pp)$ reactions. This work goes beyond that of Ref. [7], which did not address the momentum dependence of the tensor force and induced correlations, by showing important effects at relative momenta greater than 1.5 fm^{-1}. These effects, associated with small total and large relative momenta in the *NN* pair, cannot be computed within the $v_{\text{low } k}$ framework [8] directly, but require the inclusion of additional many-body, nonlocal, spin-isospin dependent operators.

The probability of finding two nucleons with relative momentum $\mathbf{q}$ and total momentum $\mathbf{Q}$ in isospin state TM_T in the ground state of a nucleus is proportional to the density

$$\rho_{TM_T}(\mathbf{q}, \mathbf{Q}) = \frac{A(A-1)}{2(2J+1)} \sum_{M_J} \int d\mathbf{r}_1 d\mathbf{r}_2 d\mathbf{r}_3 \cdots d\mathbf{r}_A d\mathbf{r}_1' d\mathbf{r}_2' \psi_{JM_J}^\dagger(\mathbf{r}_1', \mathbf{r}_2', \mathbf{r}_3, \ldots, \mathbf{r}_A) e^{-i\mathbf{q}\cdot(\mathbf{r}_{12}-\mathbf{r}_{12}')} e^{-i\mathbf{Q}\cdot(\mathbf{R}_{12}-\mathbf{R}_{12}')}$$

$$\times P_{TM_T}(12)\psi_{JM_J}(\mathbf{r}_1, \mathbf{r}_2, \mathbf{r}_3, \ldots, \mathbf{r}_A), \tag{1}$$

where $\mathbf{r}_{12} \equiv \mathbf{r}_1 - \mathbf{r}_2$, $\mathbf{R}_{12} \equiv (\mathbf{r}_1 + \mathbf{r}_2)/2$, and similarly for $\mathbf{r}_{12}'$ and $\mathbf{R}_{12}'$. $P_{TM_T}(12)$ is the isospin projection operator, and ψ_{JM_J} denotes the nuclear wave function in spin and spin-projection state JM_J. The normalization is

$$\int \frac{d\mathbf{q}}{(2\pi)^3} \frac{d\mathbf{Q}}{(2\pi)^3} \rho_{TM_T}(\mathbf{q}, \mathbf{Q}) = N_{TM_T}, \tag{2}$$

where N_{TM_T} is the number of *NN* pairs in state TM_T.

Obviously, integrating $\rho_{TM_T}(\mathbf{q}, \mathbf{Q})$ over only $\mathbf{Q}$ gives the probability of finding two nucleons with relative momentum $\mathbf{q}$, regardless of their pair momentum $\mathbf{Q}$ (and vice versa).

The present study of two-nucleon momentum distributions in light nuclei (up to $A = 8$) is based on variational Monte Carlo (VMC) wave functions, derived from a realistic Hamiltonian consisting of the Argonne v_{18} two-

nucleon [9] and Urbana-IX three-nucleon [10] interactions
(AV18/UIX). The high accuracy of the VMC wave functions is well documented (see Refs. [11,12] and references
therein), as is the quality of the AV18/UIX Hamiltonian in
quantitatively accounting for a wide variety of light nuclei properties, such as elastic and inelastic electromagnetic form factors [13], and low-energy capture reactions [14]. However, it is important to stress that the
large effect of tensor correlations on two-nucleon momentum distributions and the resulting isospin dependence of the latter remain valid, even if one uses a semi-

realistic Hamiltonian model. This will be shown explicitly
below.

The double Fourier transform in Eq. (1) is computed by
Monte Carlo (MC) integration. A standard Metropolis
walk, guided by $|\psi_{JM_J}(\mathbf{r}_1, \mathbf{r}_2, \mathbf{r}_3, \ldots, \mathbf{r}_A)|^2$, is used to sample configurations [12]. For each configuration a two-dimensional grid of Gauss-Legendre points, x_i and X_j, is
used to compute the Fourier transform. Instead of just
moving the ψ' position ($\mathbf{r}'_{12}$ and $\mathbf{R}'_{12}$) away from a fixed
ψ position ($\mathbf{r}_{12}$ and $\mathbf{R}_{12}$), both positions are moved symmetrically away from $\mathbf{r}_{12}$ and $\mathbf{R}_{12}$, so Eq. (1) becomes

$$\rho_{TM_T}(\mathbf{q}, \mathbf{Q}) = \frac{A(A-1)}{2(2J+1)} \sum_{M_J} \int d\mathbf{r}_1 d\mathbf{r}_2 d\mathbf{r}_3 \cdots d\mathbf{r}_A d\mathbf{x} d\mathbf{X} \psi^\dagger_{JM_J}(\mathbf{r}_{12} + \mathbf{x}/2, \mathbf{R}_{12}$$

$$+ \mathbf{X}/2, \mathbf{r}_3, \ldots, \mathbf{r}_A)e^{-i\mathbf{q}\cdot\mathbf{x}}e^{-i\mathbf{Q}\cdot\mathbf{X}}P_{TM_T}(12)\psi_{JM_J}(\mathbf{r}_{12} - \mathbf{x}/2, \mathbf{R}_{12} - \mathbf{X}/2, \mathbf{r}_3, \ldots, \mathbf{r}_A). \quad (3)$$

Here the polar angles of the x and X grids are also sampled
by MC integration, with one sample per pair. This procedure is similar to that adopted most recently in studies of
the $^3\mathrm{He}(e, e'p)d$ and $^4\mathrm{He}(\vec{e}, e'\vec{p})^3H$ reactions [15] and has
the advantage of very substantially reducing the statistical
errors originating from the rapidly oscillating nature of the
integrand for large values of q and Q. Indeed, earlier
calculations of nucleon and cluster momentum distributions in few-nucleon systems, which were carried out by
direct MC integration over all coordinates, were very noisy
for momenta beyond 2 fm^{-1}, even when the random walk
consisted of a very large number of configurations [2].

The present method is, however, computationally intensive, because complete Gaussian integrations have to be
performed for each of the configurations sampled in the
random walk. The large range of values of x and X required
to obtain converged results, especially for ^{3}He, require
fairly large numbers of points; we used grids of up to 96
and 80 points for x and X, respectively. We also sum over
all pairs instead of just pair 12.

The np and pp momentum distributions in ^{3}He, ^{4}He,
^{6}Li, and ^{8}Be nuclei are shown in Fig. 1 as functions of the
relative momentum q at fixed total pair momentum $Q = 0$,
corresponding to nucleons moving back to back. The statistical errors due to the Monte Carlo integration are displayed only for the pp pairs; they are negligibly small for
the np pairs. The striking features seen in all cases are
(i) the momentum distribution of np pairs is much larger
than that of pp pairs for relative momenta in the range
1.5–3.0 fm^{-1}, and (ii) for the helium and lithium isotopes
the node in the pp momentum distribution is absent in the
np one, which instead exhibits a change of slope at a
characteristic value of $p \simeq 1.5$ fm^{-1}. The nodal structure
is much less prominent in ^{8}Be. At small values of q the
ratios of np to pp momentum distributions are closer to
those of np to pp pair numbers, which in ^{3}He, ^{4}He, ^{6}Li,
and ^{8}Be are, respectively, 2, 4, 3, and 8/3. Note that the np
momentum distribution is given by the linear combination

$\rho_{TM_T=10} + \rho_{TM_T=00}$, while the pp momentum distribution
corresponds to $\rho_{TM_T=11}$. The wave functions utilized in the
present study are eigenstates of total isospin (1/2 for ^{3}He,
and 0 for ^{4}He, ^{6}Li, and ^{8}Be), so the small effects of isospin-symmetry-breaking interactions are ignored. As a result, in
^{4}He, ^{6}Li, and ^{8}Be the ρ_{TM_T} is independent of the isospin
projection and, in particular, the pp and $T = 1$ np momentum distributions are the same.

The excess strength in the np momentum distribution is
due to the strong correlations induced by tensor components in the underlying NN potential. For $Q = 0$, the pair
and residual $(A - 2)$ system are in a relative S wave. In ^{3}He
and ^{4}He with uncorrelated wave functions, 3/4 of the np
pairs are in deuteronlike $T, S = 0, 1$ states, while the pp,
nn, and remaining 1/4 of np pairs are in $T, S = 1, 0$
(quasibound) states. When multibody tensor correlations
are taken into account, 10%–15% of the $T, S = 1, 0$ pairs
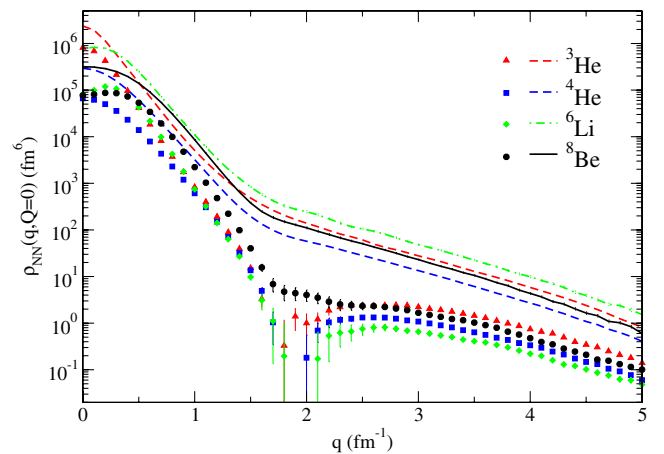are spin flipped to $T, S = 1, 1$ pairs, but the number of

FIG. 1 (color online). The np (lines) and pp (symbols) momentum distributions in various nuclei as functions of the
relative momentum q at vanishing total pair momentum Q.

$T, S = 0, 1$ pairs hardly changes [1]. In $A > 4$ nuclei, some np and pp pairs will be in relative P waves ($T, S = 1, 1$, and 0,0) when one particle is in the s shell and one in the p shell. Nevertheless, 5.5 out of 9 np pairs in ^{6}Li (9 out of 16 in ^{8}Be) are expected to be deuteronlike, while half the pp pairs will be in $T, S = 1, 0$ states and half in $T, S = 1, 1$ states [16]. The tensor force vanishes in the former and is weak in the latter.

These expectations are born out by our calculations, as Fig. 1 clearly demonstrates. The np momentum distributions for q values larger than 1.5 fm^{-1} only differ by a scaling factor, and indeed all scale relative to the deuteron momentum distribution as shown in Fig. 2. The deuteron $\rho_{np}(q, Q = 0)$ has been scaled to match that of ^{4}He at $q = 1.5$ fm^{-1}. (The scaling property does not extend to the low q region, because there binding effects take over.) The S- and D-wave components of the deuteron density are also shown in the figure as dotted lines; the D-state component is the dominant part over the range 1.4–4.0 fm^{-1}, while the S-state component has a node at 2.1 fm^{-1}.

Similar considerations in relation to scaling and binding effects also remain valid when considering the pp momentum distributions. In particular, the node seen in helium and lithium is reminiscent of the node in the S-wave momentum distribution (shown in Fig. 2). In larger nuclei the node is filled in, due to the fact that pp pairs are not exclusively in quasibound states, but can also be in P-wave or higher partial-wave states.

Figure 2 also shows the np and pp momentum distributions in ^{4}He obtained with Hamiltonians of decreasing sophistication, ranging from the fully realistic AV18/UIX model to the semirealistic Argonne v_6' (AV6$'$) to the relatively simple Argonne v_4' (AV4$'$). The AV4$'$ and AV6$'$ potentials are constructed to preserve as many features of
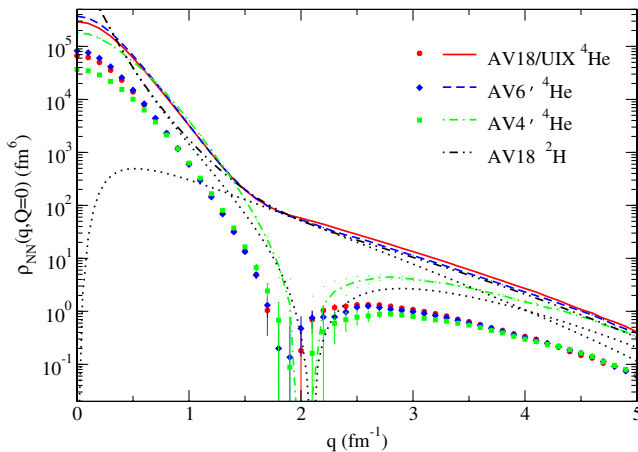
NN scattering and deuteron properties as feasible [7]. The AV4$'$ has only central, spin, and isospin operators with no tensor component: it reproduces the $^1S_0$ phase shift, and the deuteron binding energy but with only an S-state component; the D state, induced by the tensor term in the potential and associated with one-pion exchange at long range, is absent. On the other hand, the AV6$'$ includes tensor terms and produces a bound deuteron quite close to that of AV18. These features of the underlying NN potential, or the lack of them, are reflected in the calculated momentum distributions. In particular, note the node which develops in the AV4$'$ np momentum distribution, due to the purely S-wave nature of the deuteronlike state. On the other hand, the AV6$'$ and AV18/UIX results are very close to each other, demonstrating the essential role played by the tensor potential in substantially increasing the intermediate-momentum components of np pairs.

The momentum distributions $\rho_{NN}(q)$ and $\rho_{NN}(Q)$ obtained by integrating over Q or q, respectively, are plotted in Fig. 3 for ^{4}He with the AV18/UIX Hamiltonian. There is no node in $\rho_{pp}(q)$: it is filled in by the contributions of pp channels other than $^1S_0$. These channels are now allowed, because the orbital angular momentum between the pp pair and the residual nn cluster is not constrained to vanish for $Q > 0$. A remnant of the strong tensor correlations affecting $\rho_{np}(q)$ still persists. This is illustrated in the inset of Fig. 3, which shows the ratio $\rho_{np}(q)/\rho_{pp}(q)$. However, the effect is far less dramatic than in the back-to-back ($Q = 0$) kinematics. Note that $\rho_{NN}(q)$ and $\rho_{NN}(Q)$ have the same normalization, i.e., $(A - Z)Z$ for np and $Z(Z - 1)/2$ for pp. The $\rho_{np}(Q)/\rho_{pp}(Q)$ ratio is close to the np to pp pair number ratio—four in ^{4}He—over the whole range of Q values. This holds true for all the nuclei studied.

The most direct evidence for tensor correlations in nuclei comes from measurements of the deuteron structure
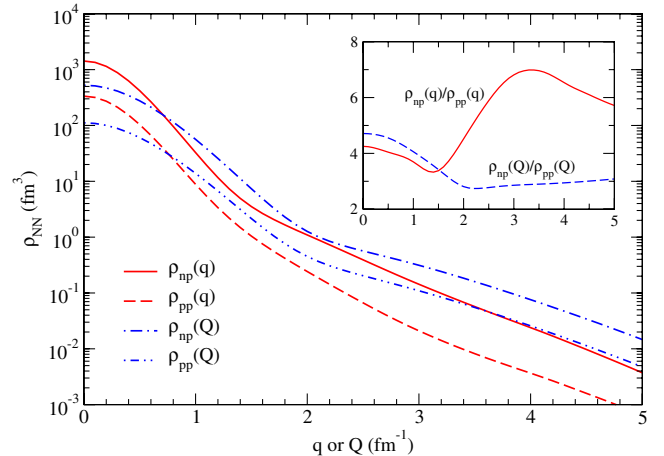

FIG. 2 (color online). The np (lines) and pp (symbols) momentum distributions in ^{4}He obtained with different Hamiltonians. Also shown is the scaled momentum distribution for the AV18 deuteron; its separate S- and D-wave components are shown by dotted lines.

FIG. 3 (color online). The momentum distributions $\rho_{NN}(q)$ and $\rho_{NN}(Q)$ in ^{4}He for np and pp. The inset shows the ratios $\rho_{np}(q)/\rho_{pp}(q)$ and $\rho_{np}(Q)/\rho_{pp}(Q)$.

functions and tensor polarization by elastic electron scattering [17]. In essence, these measurements have mapped out the Fourier transforms of the charge densities of the deuteron in states with spin projections ± 1 and 0, showing that they are very different. In other processes, such as ^{2}H$(d, \gamma)^4$He [18] at very low energy, or proton knockout from a polarized deuteron [19] (as well as in the nuclear properties mentioned at the beginning of this Letter), the effects of tensor correlations are more subtle and their presence is not easily isolated in the experimental data. This is because of ''contaminations'' from initial or final state interactions and many-body terms in the transition operators.

Some of these corrections will also pollute the cross sections for $(e, e'np)$ and $(e, e'pp)$, or (p, pp) and (p, ppn), knockout processes in back-to-back kinematics. However, one would expect the contributions due to final state interactions in the np and pp reactions, both between the nucleons in the pair and between these and the nucleons in the residual $(A - 2)$ system, to be of similar magnitude for relative momenta in the range (300–600) MeV/c. In the electrodisintegration processes, the leading electromagnetic two-body currents associated with pion and ρ-meson exchange, denoted, respectively, as PS and V in Ref. [20], vanish in pp because of their isospin structure. Of course, they will contribute in np, but are not expected to produce large effects. Thus the np cross section should be at least an order of magnitude larger than the pp for relative momenta within (300–600) MeV/c, reflecting the large difference between the corresponding momentum distributions in this range. There are strong indications from a recent analysis of a Brookhaven National Laboratory experiment, which measured cross sections for (p, pp) and (p, ppn) processes on ^{12}C in kinematics close to 2 nucleons being ejected back to back, that this is indeed the case [21]. The ratio of (p, ppn) to (p, pp) events over the range of relative momenta (275–550) MeV/c is found to be roughly 20, albeit with a rather large error. Hopefully, a more precise value for this ratio will become available in the near future, when the analysis of ^{12}C$(e, e'np)$ and ^{12}C$(e, e'pp)$ data, taken at Jefferson Laboratory, is completed [22].

It would be interesting to extend these measurements to other nuclei. In ^{3}He and ^{4}He, one would expect the node in the pp momentum distribution to be filled in by interaction effects in the final state [15]. However, the ratio of np to pp cross sections in the range (300–600) MeV/c should still reflect the large value of the np momentum distribution at these values of relative momenta. This would pro-vide a further, direct verification of the crucial role that the tensor force plays in shaping the short-range structure of nuclei.

[1] J. L. Forest *et al.*, Phys. Rev. C **54**, 646 (1996).
[2] R. Schiavilla, V. R. Pandharipande, and R. B. Wiringa, Nucl. Phys. **A449**, 219 (1986).
[3] S. C. Pieper, R. B. Wiringa, and V. R. Pandharipande, Phys. Rev. C **46**, 1741 (1992).
[4] O. Benhar, A. Fabrocini, and S. Fantoni, Nucl. Phys. **A505**, 267 (1989).
[5] A. Fabrocini and S. Fantoni, Nucl. Phys. **A503**, 375 (1989).
[6] V. R. Pandharipande *et al.*, Phys. Rev. C **49**, 789 (1994).
[7] R. B. Wiringa and S. C. Pieper, Phys. Rev. Lett. **89**, 182501 (2002).
[8] S. K. Bogner, R. J. Furnstahl, R. J. Perry, and A. Schwenk, nucl-th/0701013.
[9] R. B. Wiringa, V. G. J. Stoks, and R. Schiavilla, Phys. Rev. C **51**, 38 (1995).
[10] B. S. Pudliner *et al.*, Phys. Rev. Lett. **74**, 4396 (1995).
[11] J. Carlson and R. Schiavilla, Rev. Mod. Phys. **70**, 743 (1998).
[12] S. C. Pieper and R. B. Wiringa, Annu. Rev. Nucl. Part. Sci. **51**, 53 (2001).
[13] R. B. Wiringa and R. Schiavilla, Phys. Rev. Lett. **81**, 4317 (1998); L. E. Marcucci, D. O. Riska, and R. Schiavilla, Phys. Rev. C **58**, 3069 (1998).
[14] L. E. Marcucci *et al.*, Nucl. Phys. **A777**, 111 (2006).
[15] R. Schiavilla *et al.*, Phys. Rev. Lett. **94**, 072303 (2005); Phys. Rev. C **72**, 064003 (2005).
[16] R. B. Wiringa, Phys. Rev. C **73**, 034317 (2006).
[17] A complete list of references is in R. Gilman and F. Gross, J. Phys. G **28**, R37 (2002).
[18] A. Arriaga, V. R. Pandharipande, and R. Schiavilla, Phys. Rev. C **43**, 983 (1991).
[19] Z.-L. Zhou *et al.*, Phys. Rev. Lett. **82**, 687 (1999); I. Passchier *et al.*, Phys. Rev. Lett. **88**, 102302 (2002).
[20] L. E. Marcucci *et al.*, Phys. Rev. C **72**, 014001 (2005).
[21] E. Piasetzky *et al.*, Phys. Rev. Lett. **97**, 162504 (2006).
[22] E. Piasetzky and D. Higinbotham (private communication).